

Search for the Standard Model Higgs Boson in ATLAS

Prolay Mal

(on behalf of the ATLAS collaboration)
SPP/IRFU, CEA Saclay, Gif-sur-Yvette 91191, France

DOI: will be assigned

The search for the Standard Model (SM) Higgs boson based on $4.7\text{-}4.9\text{ fb}^{-1}$ of pp collision data at $\sqrt{s} = 7\text{ TeV}$ recorded with the ATLAS detector is presented here. The combined ATLAS results exclude the SM Higgs boson masses (m_H) of $110.0\text{-}117.5$, $118.5\text{-}122.5$ and $129\text{-}539\text{ GeV}$ at 95% confidence level. An excess of events has been observed around $m_H \sim 126\text{ GeV}$ with the global probability of 30% (10%) to occur anywhere in $110 < m_H < 600$ ($110 < m_H < 146$) GeV.

1 Introduction

The Higgs mechanism [1] provides a general framework to explain the observed masses of the W and Z gauge bosons through electroweak symmetry breaking. Within the Standard Model (SM), this mechanism posits the existence of a scalar boson, the Higgs boson, with an a priori unknown mass (m_H). The direct searches for the SM Higgs boson at the LEP experiments have excluded $m_H < 114.4\text{ GeV}$ [2], while the searches at the Tevatron exclude $156 < m_H < 177\text{ GeV}$ [3]. However, a global fit of the electroweak measurements performed at LEP, SLD and the Tevatron experiments, predicts a SM Higgs boson mass of $94^{+29}_{-24}\text{ GeV}$.

2 Individual Search Channels

The SM Higgs searches in ATLAS have been performed over a wide range of Higgs boson masses (110-600 GeV) considering different SM production mechanisms (gluon fusion, vector boson fusion and vector boson associated production) and their subsequent decay modes. The detector resolution for the reconstructed Higgs boson mass plays a crucial role in classifying the searches into numerous channels having different selection criteria as detailed below. The SM Higgs boson signal events have been simulated using PowHeg and Pythia generators, while the background contributions have been estimated either using simulation, or directly from data as appropriate.

2.1 $H \rightarrow ZZ \rightarrow l^+l^-\nu\bar{\nu}$, $H \rightarrow ZZ \rightarrow l^+l^-q\bar{q}$, $H \rightarrow WW \rightarrow l\nu q\bar{q}'$

Searches in these channels are focused on high mass Higgs boson searches over a typical Higgs mass range of 200-600 GeV. In the ZZ channels the events are required to have a lepton pair

(e^+e^- or $\mu^+\mu^-$) with reconstructed M_{ll} close to the Z boson mass. The selected events for the $H \rightarrow ZZ \rightarrow l^+l^-\nu\bar{\nu}$ [4] search are further classified into two subcategories considering the pile-up effects ('low' and 'high') on the reconstructed missing transverse energies (\cancel{E}_T), while the $H \rightarrow ZZ \rightarrow l^+l^-\text{q}\bar{\text{q}}$ [5] search considers 'tagged' (2 b-tagged jets) and 'untagged' (< 2 b-tagged jets) events separately. Figures 1 (a) and 1 (b) show the transverse mass distribution for $H \rightarrow ZZ \rightarrow l^+l^-\nu\bar{\nu}$ candidates in the 'low' pile-up data, and $m_{l^+l^-\text{q}\bar{\text{q}}}$ distribution for $H \rightarrow ZZ \rightarrow l^+l^-\text{q}\bar{\text{q}}$ in 'tagged' selection respectively. The selection criteria for the $H \rightarrow WW \rightarrow l\nu\text{q}\bar{\text{q}}'$ search [6] are optimized over a Higgs boson mass range of 300-600 GeV considering 'H+0jet', 'H+1jet' and 'H+2jets' (mostly from the vector boson fusion processes).

2.2 $H \rightarrow ZZ^{(*)} \rightarrow l^+l^-l'^+l'^-$

The search in this channel [7] consists of event categories with different lepton flavor combinations, while the SM $ZZ^{(*)}$ production processes remain irreducible background at the final level of event selection. Full reconstruction of the Higgs boson mass is possible for this channel with excellent mass resolution (2% and 1.5% for 4e and 4 μ at $m_H \sim 120$ GeV). The 4-lepton invariant mass (m_{4l}) distribution is displayed in Figure 1 (c).

2.3 $H \rightarrow \gamma\gamma$

Although $H \rightarrow \gamma\gamma$ decays have small branching ratio (about 0.2%), search in this channel [8] has the potential to discover the Higgs boson in the low mass range (110-150 GeV). The analysis is split into nine independent sub-channels based on the photon pseudorapidity, conversion status, and the momentum component of the diphoton system transverse to the thrust axis ($p_{T\perp}$). The background distribution is obtained by fitting the $m_{\gamma\gamma}$ distribution in data with a smoothly falling exponential function, while the ATLAS $m_{\gamma\gamma}$ mass resolution is approximately 1.4% for $m_H = 120$ GeV. The diphoton invariant mass distribution is shown in Figure 1 (d).

2.4 $H \rightarrow WW^{(*)} \rightarrow l^+\nu l'^-\bar{\nu}$

The searches in this channel [9] cover a wide range of $110 < m_H < 600$ GeV consisting of different number of jets (0, 1 and 2 jets) and lepton flavor combinations (ee, $\mu\mu$ and $e\mu$) in the final states. The reconstructed WW transverse mass (m_T) has been utilized in this analysis as a discriminating variable as shown in Figure 1(e) for the 'H+0jet' sub-channel.

2.5 $(W/Z)H \rightarrow (l\nu/l^+l^-, \nu\bar{\nu})b\bar{b}$

The searches in $(W/Z)H \rightarrow (l\nu/l^+l^-, \nu\bar{\nu})b\bar{b}$ channels [10] are optimized for m_H of 110-130 GeV. The main advantage with these channels is due to the large $\text{BR}(H \rightarrow b\bar{b})$ at low m_H , along with the possibility to fully reconstruct the Higgs boson mass through $m_{b\bar{b}}$. The final states with one or two charged leptons are sub-categorized depending on the transverse momentum of the reconstructed vector boson, and the lepton flavors. Figure 1 (f) shows the $m_{b\bar{b}}$ distribution for the $WH \rightarrow l\nu b\bar{b}$ sub-channel.

2.6 $H \rightarrow \tau^+\tau^- \rightarrow l^+l^-\nu\nu\nu\nu, l\tau_{had}\nu\nu\nu, \tau_{had}\tau_{had}\nu\nu$

$H \rightarrow \tau^+\tau^-$ searches [11] consist of all possible leptonic and hadronic (τ_{had}) decay modes of the τ -leptons originating from the Higgs boson decay. For the $H \rightarrow \tau^+\tau^- \rightarrow l^+l^-\nu\nu\nu\nu$

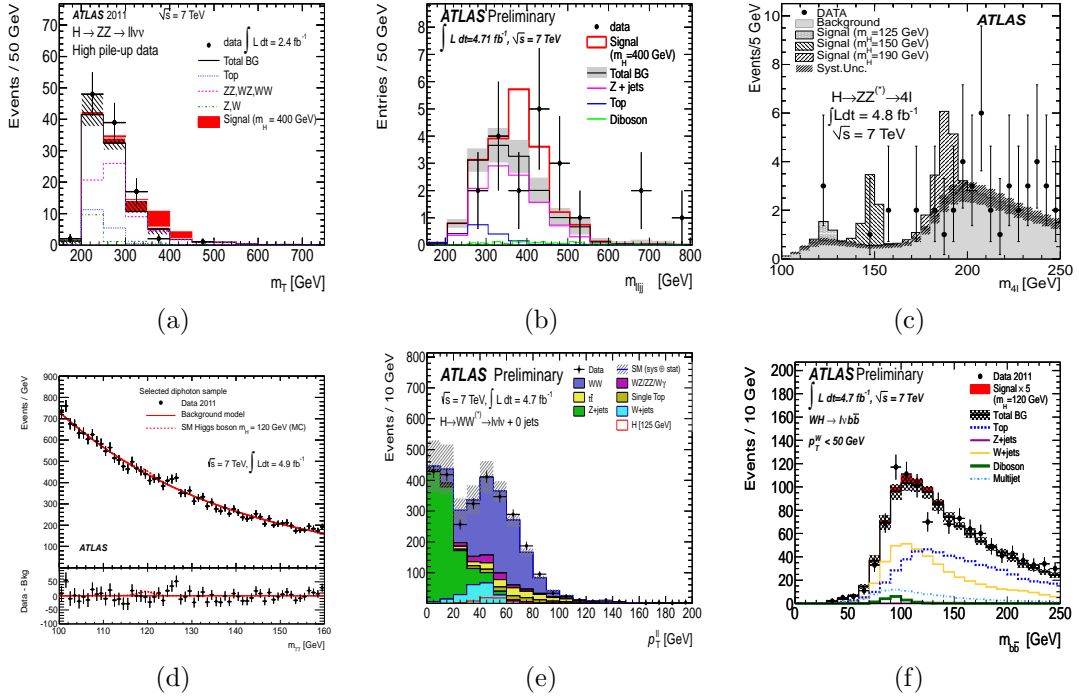


Figure 1: ATLAS SM Higgs Search observables in different channels: (a) the transverse mass distribution in $H \rightarrow ZZ \rightarrow l^+l^- \nu \bar{\nu}$ channel, (b) the invariant mass distribution of the $llqq$ system for the $H \rightarrow ZZ \rightarrow l^+l^- q \bar{q}$ search, (c) the m_{4l} distribution for the $H \rightarrow ZZ^{(*)} \rightarrow l^+l^-l'^+l'^-$ candidate events, (d) the $m_{\gamma\gamma}$ spectrum in $H \rightarrow \gamma\gamma$ search, (e) the m_T distribution in the $H \rightarrow WW^{(*)} \rightarrow l^+\nu l'^-\bar{\nu}$, and (f) the $m_{b\bar{b}}$ distribution for the $WH \rightarrow l\nu b\bar{b}$ analysis.

and $H \rightarrow \tau_{had} \tau_{had} \nu \nu$ channels, invariant mass of the $\tau^+ \tau^-$ system is reconstructed assuming collinear approximation. The searches in $H \rightarrow l \tau_{had} \nu \nu$ channel reconstruct the $m_{\tau^+ \tau^-}$ using the Missing Mass Calculator techniques [12] where the full event topology is reconstructed using the kinematics of the τ -lepton decay products.

3 Exclusion limits

The results from the aforesaid search channels have been utilized to set an upper limit on the SM Higgs boson production cross section as a function of the m_H . The limits are conveniently expressed in terms of the signal strength ($\mu = \sigma/\sigma_{SM}$), the ratio of a given Higgs boson production cross section (σ) to its SM predicted value (σ_{SM}). The CL_s prescription [13] with a profile likelihood ratio test statistic, $\lambda(\mu)$ [14] has been utilized here to derive the exclusion limits. Figure 2 shows the exclusion limits on μ at 95% confidence level (CL) for individual search channels, along with the combined ones from all search channels over the m_H range of 110-150 GeV. A small excess of events near $m_H \sim 126$ GeV is observed in $H \rightarrow \gamma\gamma$ and $H \rightarrow ZZ^{(*)} \rightarrow l^+l^-l'^+l'^-$ search channels, both of which fully reconstruct the Higgs boson mass with high resolution.

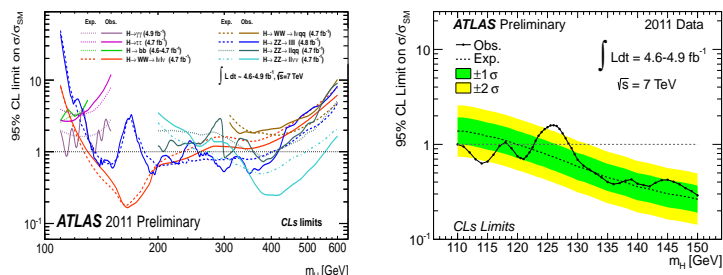


Figure 2: Exclusion limits on the SM Higgs production cross-sections at 95% CL for individual search channels (left), and for the combination of all search channels in m_H range of 110-150 GeV (right).

4 Conclusions

ATLAS has performed extensive searches for the SM Higgs boson utilizing the full 4.7-4.9 fb^{-1} dataset recorded during the 2011 LHC operations. The ATLAS combination [15] from numerous search channels excludes the SM Higgs boson mass in ranges of 110.0-117.5 GeV, 118.5-122.5 GeV, and 129-539 GeV at the 95% CL, while an exclusion of $120 \text{ GeV} < m_H < 555 \text{ GeV}$ is expected in the absence of Higgs signal. Furthermore, the exclusion limits have been recalculated at 99% CL and the SM Higgs boson over a mass range of 130-486 GeV has been excluded. The excess in the observed data has a local significance of 2.5σ , where the expected significance in the presence of a SM Higgs boson with $m_H = 126 \text{ GeV}$ is 2.9σ . The global probability for such an excess to occur across the entire SM Higgs mass range (110-600 GeV) is estimated to be 30%. However, the said probability reduces to nearly 10% if a 110-146 GeV mass range for the SM Higgs boson is considered.

References

- [1] P. Higgs, Phys. Lett. **12** 132 (1964); P. Higgs, Phys. Lett. **13** 508 (1964); P. Higgs, Phys. Rev. **145** 1156 (1966); F. Englert and R. Brout, Phys. Lett. **13** 321 (1964).
- [2] The LEP Working Group for Higgs Boson Searches, Phys. Lett. B **565** 61 (2003).
- [3] The TEVNPH Working Group, arXiv:1107.5518v2 [hep-ex] (2011).
- [4] ATLAS Collaboration, ATLAS-CONF-2012-016, <http://cdsweb.cern.ch/record/1429665>.
- [5] ATLAS Collaboration, ATLAS-CONF-2012-017, <http://cdsweb.cern.ch/record/1429666>.
- [6] ATLAS Collaboration, ATLAS-CONF-2012-018, <http://cdsweb.cern.ch/record/1429667>.
- [7] ATLAS Collaboration, Phys. Lett. B **710** 383 (2012).
- [8] ATLAS Collaboration, Phys. Rev. Lett. **108** 111803 (2012).
- [9] ATLAS Collaboration, ATLAS-CONF-2012-012, <http://cdsweb.cern.ch/record/1429660>.
- [10] ATLAS Collaboration, ATLAS-CONF-2012-015, <http://cdsweb.cern.ch/record/1429664>.
- [11] ATLAS Collaboration, ATLAS-CONF-2012-014, <http://cdsweb.cern.ch/record/1429662>.
- [12] A. Elagin *et al.*, Nucl. Instrum. Meth. **A654** 481 (2011), arXiv:1012.4686 [hep-ex].
- [13] A. Read, J. Phys. **G28** 2693 (2002).
- [14] G. Cowan *et al.*, Eur. Phys. J. **C71** 1554 (2011).
- [15] ATLAS Collaboration, ATLAS-CONF-2012-019, <http://cdsweb.cern.ch/record/1430033>.